This article has been accepted for publication in a future issue of this journal, but has not been fully edited. Content may change prior to final publication. Citation information: DOI 10.1109/TNS.2019.2946725, IEEE Transactions on Nuclear Science

GaAs as a bright cryogenic scintillator for the detection of low-energy electron recoils from MeV/c^2 dark matter

S. Vasiukov, F. Chiossi, C. Braggio, G. Carugno, F. Moretti, E. Bourret and S. Derenzo

***Abstract* — This paper presents measurements of the luminescence and scintillation under X-ray of undoped, Si-doped, and Si, B co-doped GaAs samples at cryogenic temperature over a wide infrared (IR) region using Si and InGaAs photodetectors. The undoped GaAs has a narrow emission band at 838 nm (1.48 eV) and a low light output of about 2 ph/keV. The GaAs:Si has three broad luminescence bands at 830 nm (1.49 eV), 1070 nm (1.16 eV), 1335 nm (0.93 eV) and a light output of about 67 ph/keV. GaAs:(Si, B) has four luminescence bands at 860 nm (1.44 eV), 930 nm (1.33 eV), 1070 nm (1.16 eV) and 1335 nm (0.93 eV) with a light yield of approximately 119 ph/keV. With advances in photodetection, GaAs promises to be a useful cryogenic scintillator for the detection of electron recoils from MeV/c^2 dark matter.**

***Index Terms* — Gallium Arsenide, Dark Matter, Inorganic Scintillators, Semiconductor Scintillators, Luminescence, Radioluminescence.**

I. INTRODUCTION

Large-scale experimental searches using established scintillators (e.g. liquid xenon, liquid argon, NaI(Tl), $CaWO_4$) to detect nuclear recoils from dark matter particles in the GeV/c^2 mass range have not detected a universally accepted signal. This has motivated approaches for the detection of dark matter in the MeV/c^2 mass range, using electron recoils in semiconductors and scintillators [1-4].

Gallium Arsenide (GaAs) was identified as a promising cryogenic scintillator for the detection of MeV/c^2 mass dark matter and many of its scintillation characteristics were reported in [5]. These measurements showed that GaAs doped with silicon and boron has good scintillation luminosity (as high as 43 ph/keV), and potentially no afterglow. Two emission bands at 850 nm and 930 nm were observed using an emission spectrometer with a silicon image sensor sensitive from 250 nm to 970 nm. The work presented in this paper was motivated by the need to extend measurements of the scintillation emissions to include the 1050 nm and 1300 nm bands seen in photoluminescence experiments [6-7]. It presents the first measurements of the light yields and emission spectra of undoped GaAs, GaAs(Si) and co-doped GaAs(Si,B) at low temperature over the entire range from 800 nm to 1700 nm using Si and InGaAs photodetectors. By extending the wavelength range, a luminosity of 119 photons/keV was measured for GaAs:(Si, B).

GaAs has several advantages for the detection of electron recoils from light dark matter interactions: (1) it is commercially grown as kg-mass, high-quality crystals, (2) it is easily doped with silicon donor and boron acceptor atoms to produce a useful scintillator, (3) above $8 \times 10^{15}/cm^3$ the delocalized donor electrons necessary for radiative recombination do not freeze out [5], (4) metastable radiative states that could cause afterglow are annihilated by the delocalized electrons [5], and (5) the low band gap of 1.5 eV allows the detection of electron recoils from dark matter as light as a few MeV/c^2 [4].

II. EXPERIMENTAL DETAILS

A. GaAs Samples

Table I lists the GaAs samples used in the measurements. All samples are 450-500 µm thick, cut from crystals grown by the vertical gradient freeze (VGF) method and polished on one side.

TABLE I
GALLIUM ARSENIDE SAMPLES USED IN THIS WORK

Sample	Supplier	Si ppm	B ppm	free carriers/cm^3	Notes
GaAs:(Si, B)	AXT Inc	8.9	9.7	5.5×10^{17}	No 13316 see [5]
GaAs:Si	Wafer technology LTD	6	-	2.5×10^{18}	
GaAs (pure)	Wafer technology LTD	-	-	3×10^{7}	

B. Cryostat

All measurements were performed at 10 K using a closed-cycle Leybold-Heraeus helium cryostat.

S. Vasiukov (vasyukov_sergey@yahoo.com), F. Chiossi, C. Braggio, G. Carugno are with the Department of Physics and Astronomy, University of Padua and Istituto Nazionale Fisica Nucleare, sez. Padova via F-Marzolo 8, I-35131 Padua, Italy

F. Moretti, E. Bourret are with the Materials Sciences Division, Lawrence Berkeley National Laboratory, 1 Cyclotron Road, Berkeley, California 94720, USA

S. Derenzo is with the Molecular Biophysics and Integrated Bioimaging Division, Lawrence Berkeley National Laboratory, 1 Cyclotron Road, Berkeley, California 94720, USA

This article has been accepted for publication in a future issue of this journal, but has not been fully edited. Content may change prior to final publication. Citation information: DOI 10.1109/TNS.2019.2946725, IEEE Transactions on Nuclear Science

C. *X-ray Source*

X-rays were provided by a tungsten anode OCX/70-G tube (Compagnia Elettronica Italiana (C.E.I.)) operated at 65 kV from a HCP 70–65000 power supply (FuG Elektronik GmbH). The current was varied between 0 and 0.65 mA.

D. *Experimental Apparatus*

A schematic of the experimental apparatus is shown in Fig. 1. The 65 keVp X-ray beam passes through a thin Teflon plate (1), is collimated by an aluminum disk (2) and irradiates the GaAs sample (3). The sample (3) is mounted with the polished side facing the X-ray source between disk (2) and copper masks (4). A copper holder (5) with a 4.3 mm hole provides thermal contact with the refrigerator. Scintillation light from the sample exits the cryostat (6) as it passes through a sapphire window (7) 5 mm thick and 25 mm in diameter. The scintillation light passes through a quartz light guide (8) wrapped with several layers of a reflective Teflon film and is detected by a photodetector (9) that is either a spectrometer (section II E) or a PIN photodiode (section II F). The optical components are dry-coupled.

The quartz light guide (8) is 100 mm long and 10 mm in diameter. A 200 mm x 200 mm lead wall 25 mm thick was placed between the cryostat (6) and the photodetector (9), with a 10 mm diameter hole for the quartz light guide (8). These shielded the photodiodes from the X-ray source so no increase in photodiode current was detected when the X-ray source was turned on.

E. *X-ray Luminescence Spectrometer*

A Thorlabs CCS 175 spectrometer with a Silicon CCD detects scintillation photons from 500 to 1000 nm. An Ocean Optics NIRQuest 512 spectrometer with an InGaAs 512 element linear array covers the range from 900 to 1700 nm. The spectral resolution of the two instruments are about 0.5 and 5 nm for the Si CCD and the InGaAs array, respectively. Response curves provided by the manufacturers were used in data processing.

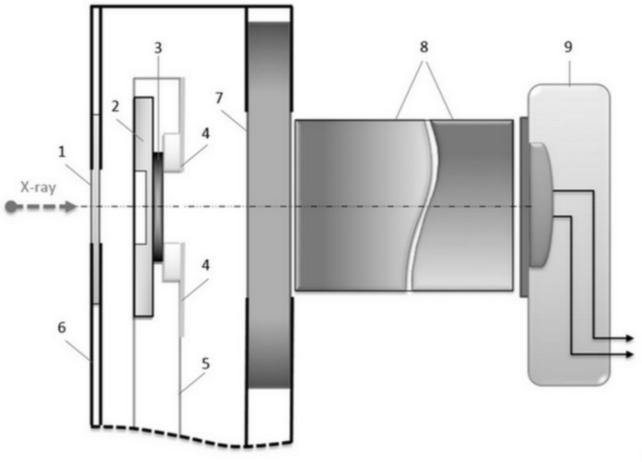

Fig. 1. The scheme of experimental equipment for light yield estimation. The description is in the text.

F. *Photodiodes and Light Yield Estimation*

A Hamamatsu S11499-01 Si PIN photodiode covers the 360-1140 nm range and was operated at room temperature. A Hamamatsu G12180-250A InGaAs PIN diode covers the 900-1700 nm range and has two-stages of thermoelectric cooling to reduce the dark current. The dark currents are 0.1 nA for the Si photodiode and 0.01 nA for the cooled InGaAs photodiode. Both photodiodes have 5 mm diameter photosensitive areas.

Photodiode currents were measured with a KEITHLEY 485 picoammeter and were used to estimate the charges that were created by the sample light emission in the PIN photodiodes. The equation for the light output calculation is:

$$LY = \frac{4\pi\, Q}{e\, \eta_\lambda\, E_R\, \Delta\Omega\, F_\lambda} = \frac{4\pi\, Q\, d^2}{e\, \eta_\lambda\, E_R\, A\, F_\lambda}, \qquad (1)$$

where Q is the charge produced in the PIN photodetector; e is the elementary charge; η_λ – the photodetector quantum efficiency in the range of the wavelength λ; E_R is the amount of the energy released in the sample by ionizing radiation (E_R=20keV); $\Delta\Omega$ – the fraction of the solid angle subtended by detector of cross sectional area A located at distance d from the sample ($\Delta\Omega$=0,055); F_λ is a factor which depends on the transparency (T) of the optical line (filters, window etc.) in the corresponding wavelength range, light collection etc. The last parameter is not fully known, for this reason the photodiode signals were calibrated using the previously studied GaAs:(Si, B) sample that was reported in Ref. [5] at 43 ph/keV in the 800-970 nm range.

III. RESULTS AND DISCUSSION

A. *X-ray Excited Emission Spectra*

Fig. 2 shows the X-ray luminescence spectra for the three samples listed in Table I from 800 to 1700 nm.

Only one narrow emission band at 838 nm (A band) is observed in the undoped GaAs crystals at 10K. Three emission bands at 830 nm (A band), 1070 nm (band C) and weak band at ~1300 nm (band D) are observed in GaAs:Si. Band A is considerably wider and asymmetrical in this case. Four luminescence bands at 830 nm (band A), 930 nm (band B), 1070 nm (band C), 1335 nm (band D) are clearly seen in co-doped GaAs:(Si, B). The intensity of the A band is very low compared to other samples. The obtained data are consistent with those reported in the literature [5-13]. The emission center parameters and their supposed nature are shown in Table II. In undoped GaAs the short wavelength emission peaking at 817 nm is attributed to the band-to-band transition, exciton relaxation or shallow levels (defects). In doped GaAs band-to-acceptor (~835 nm) and donor-to-acceptor (~870 nm) transitions have been observed. For simplicity, these emission peaks were collected in one group – band A. The nature and specific of these short wavelength emissions can explains the position and asymmetric shape of band A in GaAs:Si and GaAs:(Si, B) (Fig. 2). As can be seen from the experimental and literature data, the shape, intensity and peak position of the

This article has been accepted for publication in a future issue of this journal, but has not been fully edited. Content may change prior to final publication. Citation information: DOI 10.1109/TNS.2019.2946725, IEEE Transactions on Nuclear Science

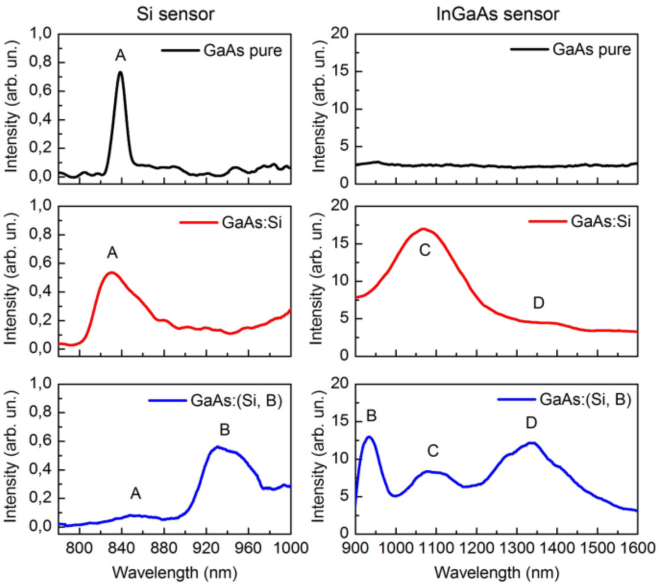

Fig. 2. The X-ray luminescence spectra at 10 K of undoped GaAs, GaAs:Si and GaAs:(Si, B) crystals obtained by Si (left column) and InGaAs (right column).

bands in 800-900 nm region in GaAs crystals drastically depends on purity, type of dopants and defects [6-10], as well as the type of conductivity [8]. The transitions from shallow silicon donors to boron acceptors on an arsenic site leads to emissions at 930 nm (band B) [5, 11, 12].

The energy relaxation on gallium vacancy-donor center leads to emission at ~1070 nm [13]. This center (band C) is a gallium vacancy (V_{Ga}) bound to a donor (like Si, Ge, Sn, C, S, Se, Te). The peak position of band C depends on the type of activator impurity.

The nature of the broad band D at ~1335 nm is associated with defects or complex centers like ($Si_{Ga} + V_{Ga} + Si_{Ga}$) or ($Si_{Ga} + Si_{As}$) and others [6, 7]. It is important to note that the formation of long-wavelength centers at ~1377 nm is observed in undoped GaAs crystals with neutron dose. The intensity of band D increases with increasing neutron dose rate, which indicates the important role of vacancies in the formation of this emission center [7].

B. Light Yield Estimation

The photodiode signals were calibrated using the previously studied GaAs:(Si,B) sample that was reported in Ref. [5] at 43 ph/keV in the 800-970 nm range. This calibration (see section II F) was used in the following sections to estimate the light output in the different emission bands for the different samples in Table I. Thorlabs shortpass (FES) and longpass (FEL) filters were used to measure the photoresponse selectively at different wavelength ranges. This makes it possible to segregate regions of a spectrum and estimate the fraction of emission bands separately in a wide range.

Fig. 3 shows the InGaAs and Si photodiode currents of the two doped samples as a function of X-ray intensity with and without filters. Table III compiles the total light output and the contribution of each emission band separately.

The results indicate a very high scintillation luminosity in activated crystals. The light yield of the GaAs:(Si, B) is 119 ph/keV. The light yield of the Si doped GaAs crystal is LY=67 ph/keV. About 60% of the total output from doped GaAs is contained in the region of 1000-1700 nm, i.e. bands C and D. This feature is dictated by the specificity of the radiative relaxation of energy in the co-doped GaAs crystal. Boron is necessary for the band B emission and this contributes to the total light output.

TABLE II
THE PARAMETERS OF RADIATIVE CENTERS IN GAAS CRYSTALS

Band	λ, nm	E, eV	Comments
A	800-870	1.42-1.54	Transition from CB to VB, exciton and shallow levels (defects)
B	933	1.33	The boron in arsenide site (B_{As} center)
C	1050-1090	1.14-1.18	Center like ($Si_{Ga} + V_{Ga}$)
D	1305-1335	0.93-0.95	Complex center like ($Si_{Ga} + V_{Ga} + Si_{Ga}$) or ($Si_{Ga} + Si_{As}$)

The output of all emission bands can vary with the dopants concentrations, for this reason the selection of a photodetector with optimal parameters is extremely important. Photodetectors that are sensitive to wavelengths above 1000 nm (e.g. Ge, InGaAs) have a clear advantage over silicon-based photodiodes that cannot detect 35 to 60% of the light emitted by GaAs:(Si, B) and GaAs:Si respectively.

GaAs has a refractive index of 3.55 at 930 nm and 3.4 at 1300 nm. Since the scintillation light is emitted isotropically, only a small fraction is able to exit the crystal directly. In this experiment, scattering within the crystal or on the roughened surface allowed a large fraction of the light to exit. Unfortunately, it is difficult to evaluate the error magnitude that

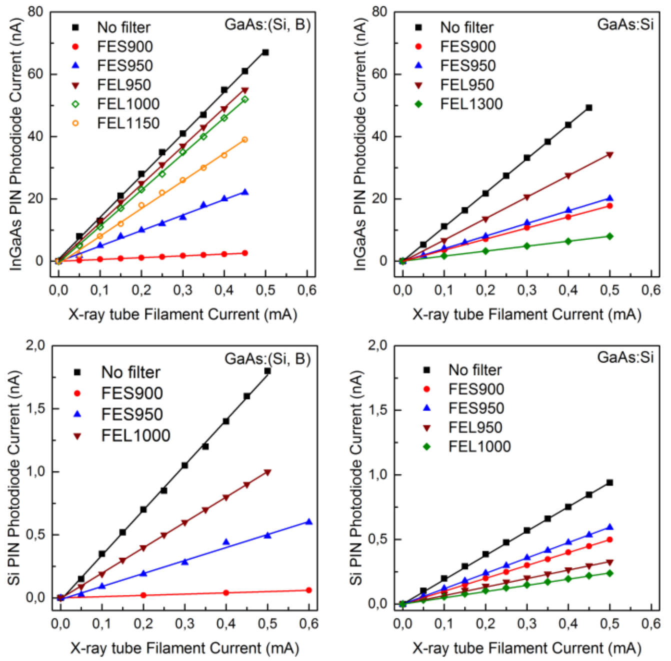

Fig. 3. The InGaAs (Top) and Si (Bottom) PIN photodiodes current dependence on X-ray filament current with/without the different shortpass (FES) and longpass (FEL) optical filters obtained on the GaAs:(Si, B) (Left) and GaAs:Si (Right) sample at 10 K.

This article has been accepted for publication in a future issue of this journal, but has not been fully edited. Content may change prior to final publication. Citation information: DOI 10.1109/TNS.2019.2946725, IEEE Transactions on Nuclear Science

TABLE III

THE LIGHT YIELD (LY) OF GALLIUM ARSENIDE SAMPLES FOR DIFFERENT SPECTRAL REGIONS AND PHOTODETECTORS

The terms correspond to equality (1): λ – wavelength, I – current, Q – charge, η – quantum efficiency, T – transparency

GaAs:(Si, B)

PD	λ (nm)	I (nA)	Q (fC)	η	T	Output	F	LY (ph/keV)	Band	LY (ph/keV)
Si	800-950	0.48	9.9	0.87	0.87	925	0,029	32	A	3
	800-900	0.046	0.9	0.88	0.85	89		3	B	40
	1000-1800	0.9	18.6	0.70	0.86	2193		76	C	76
									Total	119
InGaAs	800-900	2.5	60.3	0.20	0.9	23335	2,36	10	A	10
	800-950	20.5	494.3	0.53	0.87	75600		32	B	33
	1000-1800	52.1	1256.2	0.66	0.86	149894		63	C	21
	1150-1800	40	964.4	0.79	0.87	100332		42	D	42
									Total	106

GaAs:Si

PD	λ (nm)	I (nA)	Q (fC)	η	T	Output	F	LY (ph/keV)	Band	LY (ph/keV)
Si	800-950	0.535	11.0	0.87	0.87	1032	0.029	36	A	36
	800-900	0.448	9.2	0.88	0,85	870		30	C	24
	950-1800	0.297	6.1	0.70	0.9	692		24	Total	60
InGaAs	800-950	18.3	441.2	0.53	0.87	67487	2.36	29	A	29
	950-1800	31.2	752.3	0,66	0,9	89764		38	C	30
	1150-1800	7.3	176.0	0.79	0.88	17894		8	D	8
									Total	67

GaAs (pure)

PD	λ (nm)	I (nA)	Q (fC)	η	T	Output	F	LY (ph/keV)	Band	LY (ph/keV)
Si	800-950	0.032	0.66	0.88	0.85	62	0.029	2	A	2
									Total	2

arises, regardless of experimental methods of the LY estimation. A coating with a graded index of refraction will allow essentially all of the scintillation photons to escape directly [14].

IV. DISCUSSION AND CONCLUSIONS

We have measured X-ray excited scintillation light yields of 119 ph/keV and 67 ph/keV for GaAs:(Si, B) and GaAs:Si, respectively at 10K. The average ionization energy to produce an electron-hole pair is 4.2 eV [15]. If every pair recombined radiatively, the light yield would be 238 photons/keV. This limit could be approached by reducing the non-radiative hole traps, by optimizing the levels of Si and B, and by using antireflective coatings.

According to Ref. 5 no thermoluminescence has been detected in GaAs:(Si, B) in region 800-970 nm, indicating a likely lack of afterglow. However, the afterglow measurement in the range from 800 to 1800 nm is planned for the near future and is important for proving the complete absence of afterglow.

For detecting low-energy electron recoils from dark matter interactions, a photodetector able to detect individual IR photons with high efficiency and low dark current will be necessary. One possibility is a photon absorber (e.g. Si, Ge) that converts IR photons into athermal phonons that are detected by surface mounted superconducting transition edge sensors. This technology has been developed in the CRESST [16] and SuperCDMS [17] experiments for detecting phonons produced by dark matter interactions. Another possibility is arrays of superconducting nanowire single photon detectors that have a high quantum efficiency for IR photons. Custom lithography will be necessary to increase the photodetector area from mm^2 to cm^2.

ACKNOWLEDGMENT

The research is sponsored by Istituto Nazionale di Fisica Nucleare (INFN) within the AXIOMA project and the Office of

Basic Energy Sciences of the U.S. Department of Energy at the Lawrence Berkeley National Laboratory under UC-DOE Contract No. DE-AC02-05CH11231. The authors wish to thank Fulvio Calaon, Mario Tessaro, Mario Zago, Massimo Rebeschini, Andrea Benato and Enrico Berto for the help with cryogenics and for the mechanical and electronic work on the experimental setup.

REFERENCES

[1] R. Essig, A. Manalaysay, J. Mardon, P. Sorensen, and T. Volansky, “First direct detection limits on Sub-GeV dark matter from XENON10,” Phys. Rev. Lett. 109(2), 021301 (2012).
[2] R. Essig, J. Mardon, and T. Volansky, “Direct detection of sub-GeV dark matter,” Phys. Rev. D 85(7), 076007 (2012).
[3] R. Essig, M. Fernandez-Serra, J. Mardon, A. Soto, T. Volansky, and T. T. Yu, “Direct detection of sub-GeV dark matter with semiconductor targets,” J. High Energy Phys. 2016 (5), 46.
[4] S. Derenzo, R. Essig, A. Massari, A. Soto and Tien-Tien Yu, “Direct detection of sub-GeV dark matter with scintillating targets,” Phys. Rev. D 96, 016026 (2017).
[5] S. Derenzo, E. Bourret, S. Hanrahan, and G. Bizarri, “Cryogenic scintillation properties of n-type GaAs for the direct detection of MeV/c2 dark matter,” J. Appl. Phys. 123, 114501 (2018).
[6] H. Lei, H S Leipner, V Bondarenko and J Schreiber, “Identification of the 0.95 eV luminescence band in n-type GaAs:Si,” J. Phys.: Condens. Matter 16 (2004) S279–S285.
[7] C. Carlone, G. Bernier, E. Tannous, S.M. Khanna, W.T. Anderson, J.W. Gerdes, “The photoluminescent spectrum of neutron irradiated GaAs,” IEEE Trans Nucl. Sci., vol. 37, No6 (1990), 1718-1725.
[8] Young-Ki Ha, Ch. Lee, Jae-Eun Kim and Hae Yong Park, S. B. Kim and H. Lim, Bong-Cheol Kim, Hee-Chul Lee, “Defect Luminescence in Heavily Si-Doped n- and p-type GaAs,” J. Korean Phys. Soc., Vol. 36, No. 1, (2000), 42-48.
[9] D. Redfield, J. P. Wittke, and J. I. Pankove, “Luminescent Properties of Energy-Band-Tail States in GaAs:Si,” Phys. Rev. B, Vol 2, Number 6 (1970) 1830-1839.
[10] M. Mazumdar, S. Dhar, and Utpal Das, “Luminescence and deep level characteristics of GaAs/Si with atomic layer epitaxy grown predeposition layers,” J. Appl. Phys. 79 (11), (1996).
[11] V. Bondarenko, “Positron annihilation study of equilibrium point defects in GaAs,” Ph.D. thesis (Mathematisch-Naturwissenschaftlich-Technischen Fakultat, Martin-Luther-Universitat Halle-Wittenberg, 2003), Chap. 4.
[12] R. Leitsmann et al., “Boron-silicon complex defects in GaAs: An ab initio study,” J. Appl. Phys. 109(6), 063533 (2011).
[13] E. W. Williams, “Evidence for self-activated luminescence in GaAs: The gallium vacancy-donor center,” Phys. Rev. 168, 922–928 (1968).
[14] J. C. Zhang, L. M. Xiong, M. Fang, and H. B. He, "Wide-angle and broadband graded- refractive-index antireflection coatings," (in English), Chinese Physics B, vol. 22, no. 4, p. 044201, (2013).
[15] Giuseppe Bertuccioa) and Diego Maiocchi, “Electron-hole pair generation energy in gallium arsenide by X and γ photons” Journal of applied Physics, 92: 1248-1255 (2002).
[16] Abdelhameed et al., “First results from the CRESST-II low-mass dark matter program”, arXiv 1904:00498v1 (2019).
[17] Agnese et al. “First Dark Matter Constraints from SuperCDMS Single-Charge Sensitive Detectors”, arXiv 1804:10697v2 (2018).